Contact Lens and Anterior Eye xxx (xxxx) xxx

Contents lists available at ScienceDirect

Contact Lens and Anterior Eye

journal homepage: www.elsevier.com/locate/clae

Optical simulations of the impact of vault increase in scleral contact lenses in healthy eyes

David P. Piñero [a,b,*], Ángel Tolosa [a,c], Miguel A. Ariza-Gracia [d]

[a] Department of Optics, Pharmacology and Anatomy, University of Alicante, Alicante, Spain
[b] Department of Ophthalmology, Vithas Medimar International Hospital, Alicante, Spain
[c] Doitplenoptic, S.L., Paterna, Spain
[d] ARTORG Center for Biomedical Engineering Research, University of Bern, Bern, Switzerland

ARTICLE INFO

Keywords:
Scleral contact lens
Spherical aberration
Vault
Ray tracing
Vergence

ABSTRACT

Purpose: To investigate by using computational simulations the optical impact of the change in the vault of two geometries of scleral contact lenses (SCLs).
Methods: Ray-tracing simulations were performed using specialized software in three eye models with different levels of primary SA (6 mm pupil). Two different geometries of SCL were used in such simulations characterized by the conic constants of the anterior surface of the lens (K1, −0.1 and −0.3). Likewise, the fitting of the SCL was simulated for different vaults (50–250 μm). The impact on the quality of the images through the eye models was assessed by analyzing the modulation transfer function (MTF) at different spatial frequencies (10 Lp/mm, 30 Lp/mm, and 50 Lp/mm). This impact was not only simulated for a distant object, but also for intermediate and near objects (vergence demands from 0.00 to 3.00 D). All these optical simulations were performed assuming a centered SCL, but also assuming a downward vertical decentration of 0.5 mm.
Results: The thinnest vault (50 μm) provided the best ocular optical quality in all three eye models for low vergence demands. For medium and high vergence demands, Lens 1 (K1 = −0.3, K2 = −0.4) resulted in a considerable improvement in optical quality in Eye 2 ($C_4^0 = -0.078$ μm), while for eyes 1 ($C_4^0 = 0.408$ μm) and 3 ($C_4^0 = -0.195$ μm), this improvement only tended to happen for medium vergence demands. Overall, all the aberrations increased after lens fitting. Lens decentration did not cause significant variations in the results obtained with the well-centered lenses.
Conclusions: Changes in the vault of a SCL have an impact on the optical quality achieved for different vergence demands independently on the level of SA of the eye in which it is fitted. The clinical relevance of such impact should be investigated further.

1. Introduction

The use of scleral contact lenses (SCLs) has grown significantly in the last years, with an exponential increase in the number of investigations on this issue [1]. Although there is a consensus about most of the aspects of SCL management among practitioners with more than 5-year experience in scleral lenses [2], there are still aspects that require of deeper research, such as the selection of the diameter of the lens, the daily wearing time, the height of the vault, the potential optical impact of the selected vault or the use of non-preserved products for lens application [3].

The tear reservoir between the posterior surface of the SCL and the anterior corneal surface is defined as the vault, which is indeed a relevant parameter to be monitored during SCL fitting [4]. Different recommendations have been provided for the selection of the vault in terms of oxygen permeability [5–8]. Compañ and colleagues[7] recommended the use of lens materials with a 125 barrier of oxygen permeability along with vaults below 150 μm. Similarly, Michaud et al. [8] recommended the use of SCLs made of material with high oxygen permeability (Dk > 150), with a central thickness of 250 μm as maximum, and vaults below 200 μm [8]. In recent clinical studies, controlled levels of corneal swelling after a daily wearing of SCLs have been reported (on average

* Corresponding author at: Department of Optics, Pharmacology and Anatomy, University of Alicante, Crta San Vicente del Raspeig s/n 03016, San Vicente del Raspeig, Alicante, Spain.
E-mail address: david.pinyero@ua.es (D.P. Piñero).

https://doi.org/10.1016/j.clae.2023.101847
Received 26 May 2022; Received in revised form 1 April 2023; Accepted 16 April 2023

<2%, [9] with some rare exceptions. [10].

Besides the impact on corneal physiology, the SCL vault may significantly affect the visual performance of the observer [11,12]. It should be considered that an increase of the SCL vault may lead to a change in its optical effect as well as a decentration of the SCL would generate an asymmetrical meniscus shape. However, very few studies have investigated the clinical impact of this potential change of the meniscus shape and thickness on ocular optical and visual performance. In a recent pilot study, the increase in the central vault when a fitting a specific type of SCL in healthy eyes was shown to be associated to a more myopic refractive error, and to an increase in different ocular HOAs [12]. In another clinical study, Otchere et al. [11] concluded that a SCL fitting that added 375 μm to the corneal sagitta (measured by optical coherence tomography, OCT) resulted in the best combination of acuity and comfort ratings. Contrarily, Sonsino and Mathe [13] did not find a correlation between the magnitude of the vault and the LogMAR visual acuity in a study that included patients fitted with SCLs with vaults ranging from 220 μm to 600 μm.

All these contradictory outcomes make it difficult to define specific recommendations about the vault selection from an optical perspective. In particular, the 'thin lens' paraxial approximation (traditionally used in the calculation of corneal rigid lenses) might not remain valid in the presence of a significantly thick tear layer between cornea and lens, leading to inaccurate results [14]. This is an aspect that needs to be clarified specially when fitting SCLs with multifocality. Multifocal SCLs are focused on the induction of spherical aberration to expand the depth of focus and the meniscus can also induce some levels of spherical aberration depending on its shape and thickness, interfering with the aberrations induced by the multifocal SCL. Despite of the fact that some commercially available models of multifocal SCLs exist, there are no clinical studies to this date reporting their outcomes for presbyopia in peer-reviewed literature. Woods et al. [15] conducted a prospective study evaluating the results of an aspheric multifocal back surface corneal rigid gas permeable (RGP) contact lens, concluding that the required aspheric geometry can be optimized for a given patient by considering his/her degree of ametropia, as well as the corneal topography.

The hypothesis of the current investigation is that the modification of the vault when fitting different geometries of SCL's in a healthy eye will impact optical quality for distance, intermediate and near vision. As a secondary hypothesis, it has been stated that the impact of changes in SCL geometry, spherical aberration of the eye and SCL decentration will also impact optical quality for different vergence demands. For testing these hypotheses, computational simulations have been done for two different geometries of SCL (anterior surface described by two different conic constants) fitted with different vaults within a range allowing maintaining the ocular surface health. The impact in optical quality of the use of such theoretical variations in terms of ocular aberrations and SCL geometry, vault and centration has been assessed by means of the analysis of the modulation transfer function (MTF). This analysis has been performed assuming different vergence demands and therefore simulating different viewing conditions. Likewise, the simulations have been done for three different healthy eye models with different levels of primary spherical aberration within the physiological range of variation of this parameter. All this analysis could be helpful to implement SCL fittings and future clinical studies.

2. Material and methods

2.1. Initial configuration

For performing the simulations of this study, an initial configuration was needed including the generation and programming of the eye and SCL models.

2.2. Generation of eye models

All ray-tracing simulations were performed using OpTaLix-Pro® software (Optenso™, Optical Engineering Software, Igling, Germany). A pupil aperture of 6 mm in diameter and light wavelength 0.5876 μm were used for such simulations. To simulate the Stiles-Crawford effect, an apodization of the intensity in the entrance pupil was performed using a Gaussian circular distribution. The grid size (number of rays) used for the calculations was 512 × 512. The wavefront error was fitted using Fringed Zernike Polynomials, a Zernike polynomial fitting in which the coefficients were arranged following a single index scheme. These coefficients were normalized and transformed to a double index scheme according to the standards for reporting the optical aberration in human eyes [16].

Three eye models were used to analyze the impact of the vault of the simulated SCLs. The Escudero-Navarro schematic eye model was used as the baseline model for the generation of these three eye models. Eye 1 used exactly the same parameters and settings than Escudero-Navarro eye model, with a positive level of primary spherical aberration of 0.408 μm (6-mm pupil). For the creation of the other two eye models (Eyes 2 and 3), the cornea was assumed to have the same curvature, conic constant and thickness as the baseline eye model and Eye 1, but different asphericity. The asphericity of each anterior corneal surface was modified by adding a perturbation to the corresponding Zernike coefficients that modify the primary and secondary spherical aberrations (see C_4 | C_2^0 and C_9| C_4^0 in Table 1). In this case, the surface sagitta was modelled with a conic section (baseline shape) plus the aspheric terms defined by a Zernike polynomial expansion in the Fringe basis (perturbation),

$$z = \frac{cr^2}{1+\sqrt{1-(K+1)c^2r^2}} + \sum_i^N C_i Z_i(\rho,\theta) \quad (1)$$

where c is the vertex curvature, K is the conic constant, $r = \sqrt{x^2+y^2}$ is the in-plane radial component (i.e., the XY distance from optical axis -z-), N is the number of Zernike coefficients, C_i is the coefficient of the Fringe Zernike polynomial Z_i, ρ is the normalized in-plane radial coordinate (ranging from 0 to 1), and θ is the azimuthal coordinate (ranging from 0 to 2π). Table 2 summarizes the paraxial optical properties of the three eye models for infinity distance viewing.

The crystalline lens of the three eye models used in the simulations was considered as a static element and, therefore, no accommodation was present. Thus, the simulations were done in the worst conditions (no ability to focus intermediate and near objects) that are equivalent to those corresponding to a presbyopic eye with minimal or null accommodative response. Therefore, the results of these calculations can be also applied to understand the potential efficacy of the presbyopic correction that can be achieved with the SCLs simulated.

2.3. Generation of SCL models

Two different SCLs were simulated by combining two different values of the conic constant of the anterior surface of the lens (K1: −0.1 and −0.3) with the same conic constant for the posterior surface (K2: −0.4). The sagitta of these surfaces was modelled using the same conic

Table 1
Fringe Zernike coefficients added to the anterior corneal surface for inducing different levels of ocular spherical aberration, where *C4* and *C*9represent the single indexed Zernike coefficients corresponding to defocus and primary spherical aberration in the Fringe basis.

Model Eye	C4(μm)	C9 (μm)
Eye 1	0	0
Eye 2	−50	−20
Eye 3	0	−25

Table 2
Optical properties of the three eye models used, including the eye optical power, P, the standardized double indexed Zernike coefficients, C_n^m for defocus (Z_2^0) and for primary and secondary spherical aberration (Z_4^0 and Z60), and the mean spherical equivalent, M.

Eye model	P (D)	C_2^0(μm)	C_4^0(μm)	C_6^0(μm)	M (D)
Eye 1	60.53	1.048	0.408	0.018	0.26
Eye 2	59.43	−0.091	−0.078	0.017	−0.26
Eye 3	60.53	4.830	−0.195	0.016	−4.08

section as the one used to model the baseline corneal shape in equation (1), disregarding the perturbation Zernike terms. The optical power of the isolated contact lens in air was calculated using the paraxial lens equation,

$$p = \frac{1}{f'} = (n_l - 1)\left(\frac{1}{R_1} - \frac{1}{R_2}\right) + \frac{(n_l - 1)t}{n_l R_1 R_2} \quad (2)$$

where f' is the focal length of the contact lens, n_l is the refractive index of the contact lens material (1.442 for a light wavelength of 0.5876 μm), t is the vertex thickness (350 μm), R_2 is the apical radius of curvature of the posterior surface (7.720 mm to match the radius of the anterior corneal surface according to the Escudero-Navarro eye[17]), and R_1 is the apical radius of the anterior surface (7.827 mm was used to drive the optical power of the contact lens to zero).

Different fitting conditions were simulated with the two models of SCL, including central vaults of 50, 100, 150, 200 and 250 μm.

2.4. Simulations of the optical impact of vault changes of centered SCLs

The metric used to simulate the optical impact of the different fittings (vaults 50–250 μm) of the two SCLs geometries simulated was the modulation transfer function (MTF) of the combined set SCL + eye model. For each eye model, SCL geometry and vault combination, simulations were performed for eight viewing distances (different vergence demands) ranging from infinity to 33.3 cm, simulating the range from far distance to near vision. Specifically, simulations were performed for the following vergence demands: 0.00, 0.17, 0.25, 0.50, 1.00, 1.50, 2.00, 2.50, and 3.00 D.

The object viewed by each eye model and for which the simulations was performed was represented by three specific spatial frequencies (10 Lp/mm, 30 Lp/mm, and 50 Lp/mm in the image space; see Fig. 1). These spatial frequencies were equivalent to an angular resolution in the object space of 10.4 arcmin, 3.5 arcmin and 2.1 arcmin respectively.

Besides the calculation of the MTF, the coefficients of the Zernike polynomials corresponding to the defocus, primary and secondary spherical aberration were calculated for each eye model, SCL geometry, and vergence demand simulated.

2.5. Simulations of the optical impact of vault changes of vertically decentered SCLs

Additional simulations were performed considering a downward vertical decentration of 0.5 mm of each lens, as this type of decentration is not uncommon with SCLs [18]. To achieve this value of vertical decentration, the vertex of the corresponding lens was rotated 3.67 degrees following the meridian section of the cornea. With this level of decentration, the MTF was calculated under the same conditions stated above.

3. Results

3.1. Optical properties of the eyes simulated

Table 2 presents the results of the optical power (P) of each eye model and the corresponding mean spherical equivalent, M, calculated from the Zernike coefficients C_2^0, C_4^0, and C_6^0 [19]. A positive defocus means that the retina is behind the plane of best-focus and a negative one that the retina is in front of the plane of best-focus. These results show that Eye 1 (baseline model) was slightly myopic, with the plane of best-focus located 0.219 mm in front of the retina which corresponds to an equivalent dioptric value close to −0.6 D; Eye 2 balanced defocus and spherical aberration in the retina, which was very close to the best focal plane, with a negligible hyperopic residual defocus of 20 μm; and Eye 3 resulted in a highly myopic defocus of almost 1 mm, which corresponds to an equivalent dioptric value close to −1.0 D.

The analysis of the optical quality (MTF) of each isolated eye (without lens fitting) for different vergence demands (Fig. 1) showed that the MTF for Eye 1 increased as the test approached towards the observer presenting a peak between 6 m and 1 m of observation distance, depending on the frequency of the test. Eye 2 presented minimal aberration for far vision and, consequently, MTF values were higher for smaller vergences. The range in which it could distinguish the three frequencies was up to 4 m. Eye 3 was very myopic and, thus, the highest MTF values were found when the test was observed at the shortest distance (33 cm). Moreover, medium and high frequencies could not be distinguished beyond 0.50 m.

The MTF behavior was further supported by the changes in the Zernike coefficients for defocus, and primary and secondary spherical aberration with the vergence demands studied in the three eyes (Fig. 2). The defocus (C_2^0) behaved as expected: it was approximately zero for vergence demands between 0.5 and 1 D for Eye 1, it was minimum at a vergence demand of 0 D for Eye 2, and it was minimum for a vergence demand between 2.5 D and 3 D for Eye 3. The primary spherical aberration (C_4^0) did not present variation for Eye 1, while for Eyes 2 and 3 the coefficients slightly decreased with increasing vergence demand. The secondary spherical aberration (C_6^0) presented a similar behavior as the primary spherical aberration with no variation for Eye 1 and a slight decrease with increasing vergence demands.

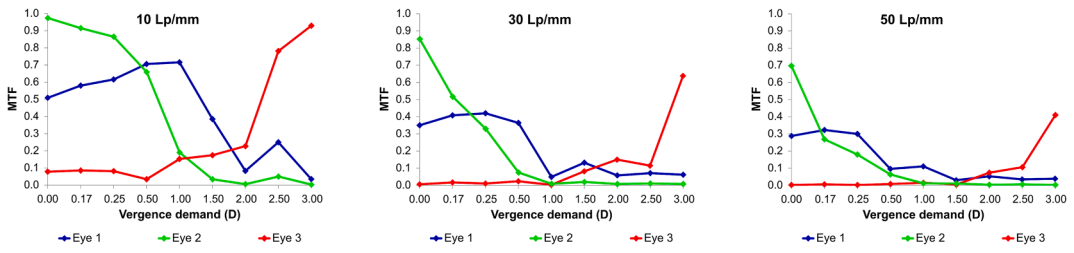

Fig. 1. Modulation transfer function (MTF) values of the three eye models evaluated in the image space at 10 Lp/mm, 30 Lp/mm, and 50 Lp/mm with no accommodation for vergence demands ranging from distance to near vision. The frequencies in the image space correspond to an angular resolution in the object space of 10.4 arcmin, 3.5 arcmin and 2.1 arcmin, respectively.

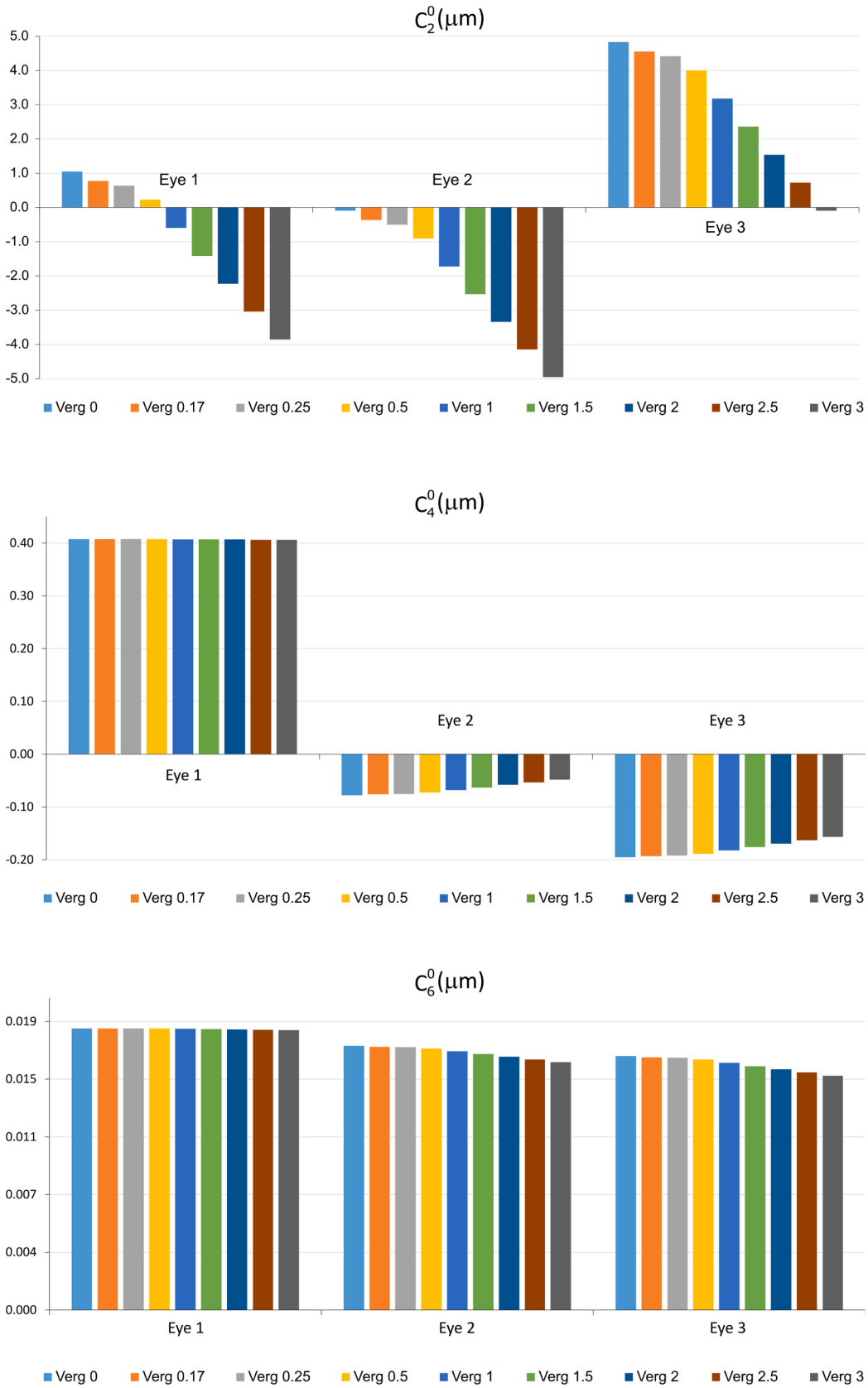

Fig. 2. Zernike coefficients for defocus and primary and secondary spherical aberration of the wavefront error of the three eye models, evaluated with no accommodation of the crystalline lens for vergence demands ranging from distance to near vision.

3.2. Simulations of the optical impact of vault changes of centered SCLs

For the sake of clarity, post-fitting simulations are presented for each lens separately (Lens 1: Figs. 3, 4 and 7; Lens 2: Figs. 5, 6 and 8). Fig. 3 presents the results of the ray-tracing in which the MTF is calculated for the different eye models and different vault magnitudes for Lens 1. After contact lens fitting, MTF values were similar for all the eyes and, therefore, Lens 1 resulted in a uniform visual behavior regardless of the pre-fitting primary and secondary spherical aberrations. For low vergence demands, the thinnest vault provided the best ocular optical quality in all three eye models. For medium and high vergence demands, Lens 1 resulted in a considerable improvement in optical quality in Eye 2, while for eyes 1 and 3, this improvement only tended to happen for medium vergence demands. In general, the thickest vaults offered better ocular optical quality for medium and high vergence demands.

Fig. 4 presents the values of the Zernike coefficients for different vergence demands. For the sake of simplicity, only the central vaults of 50 μm, 150 μm and 250 μm, and the vergence demands of 0 D, 0.25 D, 1.00 D, 2.00 D and 3.00 D are represented. Overall, all the aberrations increased after lens fitting. In this vein, the most relevant changes occurred in the defocus which increased for decreasing vaults when the vergence demand was close to 0 D, while inverting this behavior for increasing vergence demands (i.e., decreased for increasing vaults).

Fig. 5 and Fig. 6 present similar results as Fig. 3, Fig. 4 respectively, but after fitting Lens 2. In particular, Lens 2 resulted in the similar qualitative behavior as Lens 1, but with better MTF values. Likewise, the thinnest vault caused the MTF values of Eye 2 and Eye 3 to be like those of Eye 1 without the lens. With the three frequencies analyzed, the thinnest vaults provided the best results for ocular visual quality when the demand for vergence was low. Nevertheless, only Eye 3 presented corrected values above the value without the lens. Contrarily, the thickest vault resulted in the most optimized optical quality for vergence demands associated to intermediate vision (0.5 D to 1.5 D), above the baseline value of the corresponding eye with all frequencies. For high vergence demands, (between 2 D and 3 D) the best optical qualities corresponded to the thickest vaults without substantial differences except for 10 Lp/mm. This shift in the behavior suggests that there is a vergence demand threshold that must be observed carefully as the practitioner should promote thinner or thicker vaults depending on whether low vergence or high vergence are aimed to be corrected.

Fig. 6 outlines that Lens 2 presents the same behavior as Lens 1 and that there is an inversion in the impact of the vault in the ocular aberrations (for lower vergence, thinner vaults are better; for higher vergence, thicker values are better).

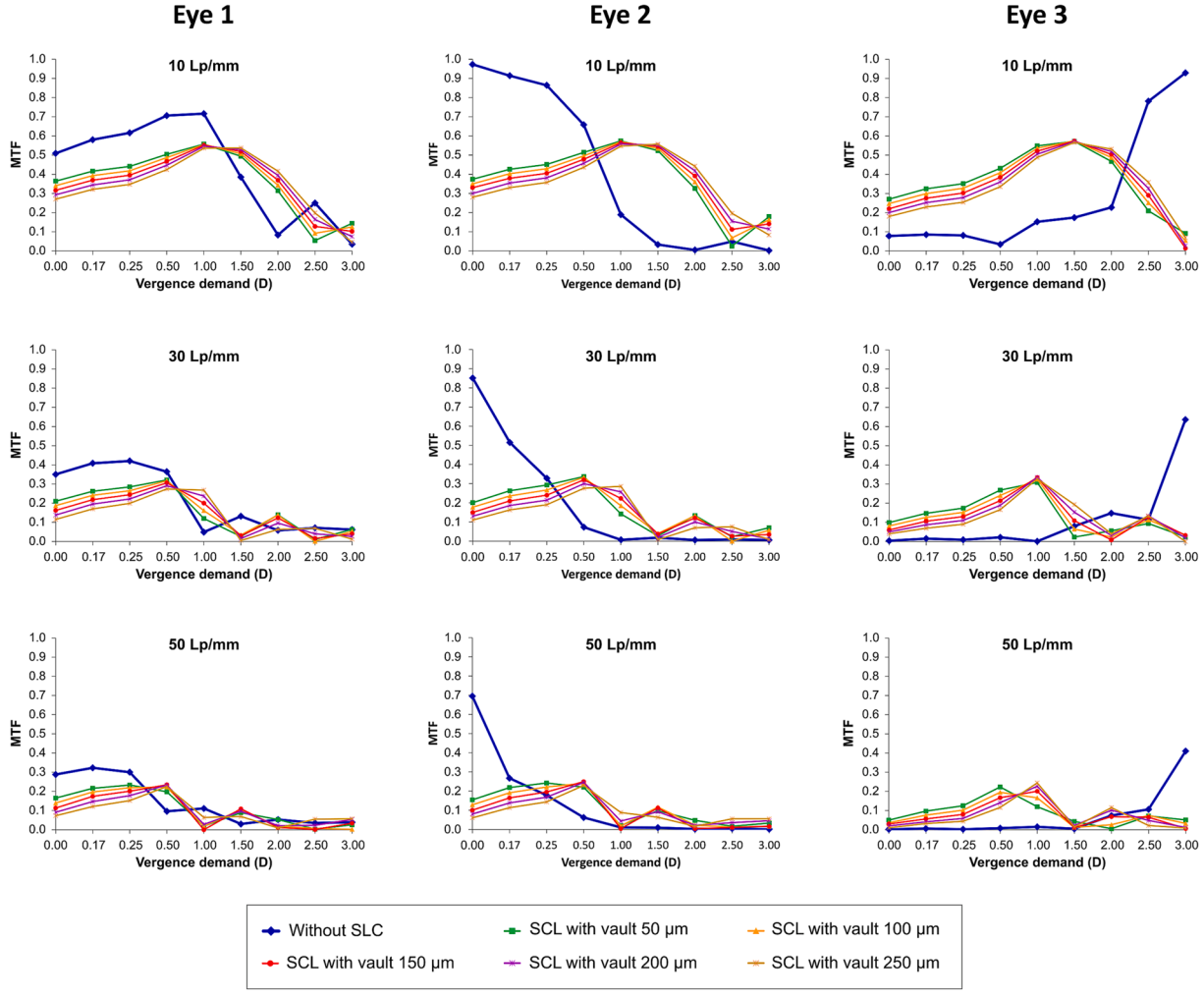

Fig. 3. Modulation transfer function values for different vergence demands after fitting the scleral contact lens 1. The MTF values were calculated for objects with spatial frequency corresponding to an angular resolution of 10.4 arcmin, 3.5 arcmin and 2.1 arcmin, respectively, and assuming a static crystalline lens position in the three eye models. Different fitting conditions were simulated of the scleral lens 1 (K1 = −0.1 and K2 = −0.4), including central vaults of 50, 100, 150, 200 and 250 μm.

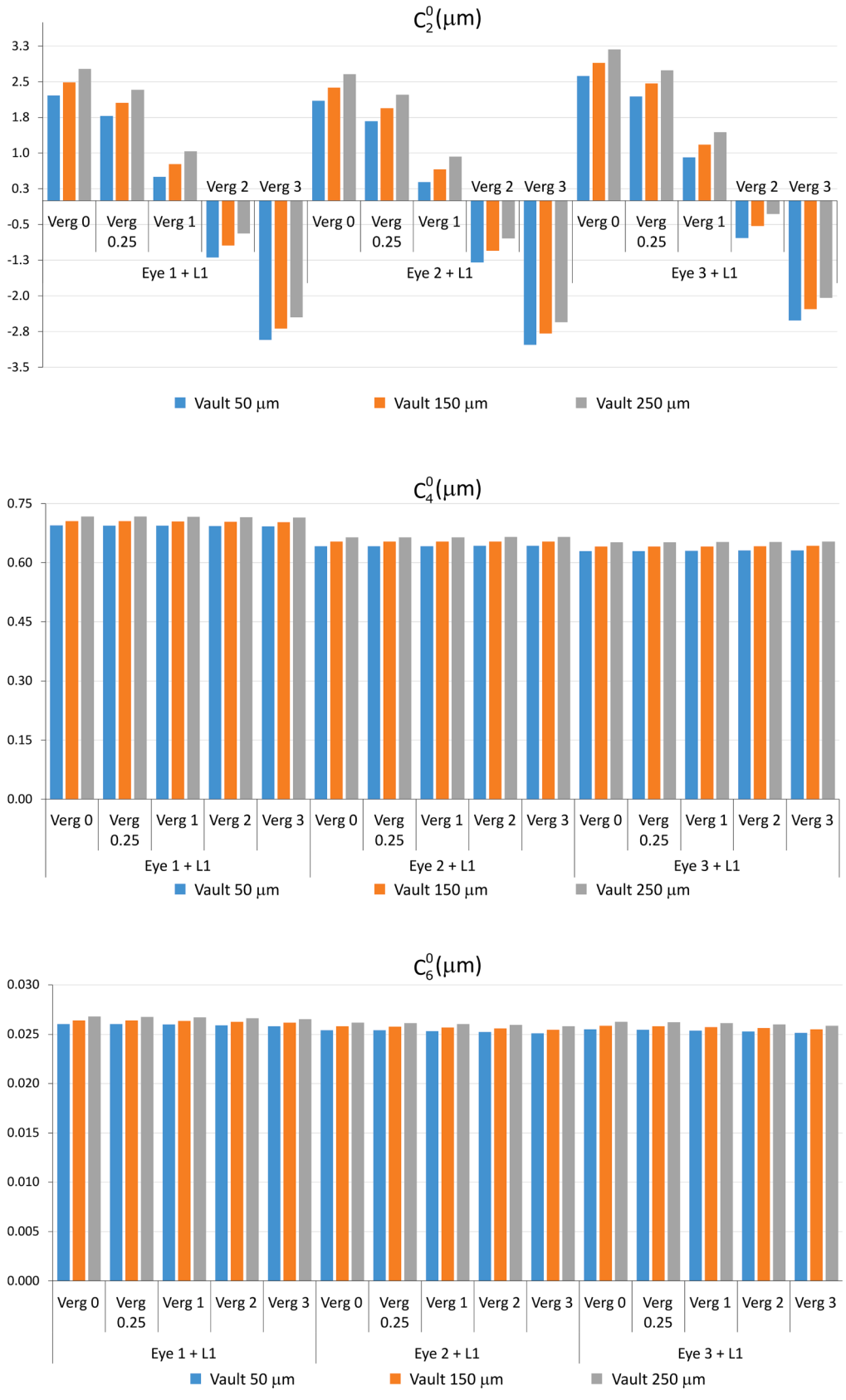

Fig. 4. Zernike coefficients for defocus and primary and secondary spherical aberration of the wavefront error after fitting the scleral contact lens 1 on the three eye models. Different central vaults of the scleral contact lens were used to evaluate the wavefront error at vergence demands ranging from distance to near vision. The crystalline lens remained static in the simulations.

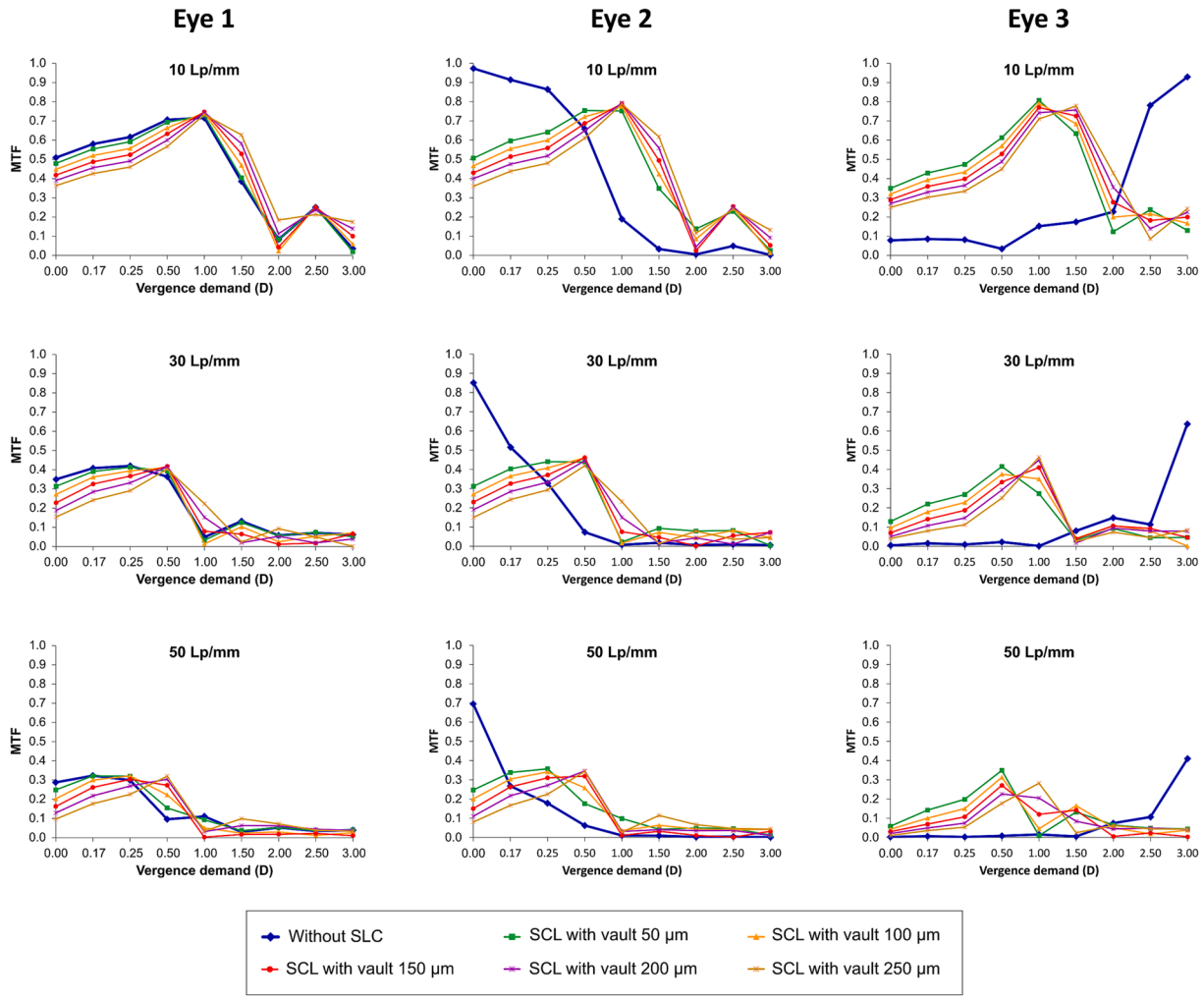

Fig. 5. Modulation transfer function values for different vergence demands after fitting the scleral contact lens 2. The MTF values were calculated for objects with spatial frequency corresponding to an angular resolution of 10.4 arcmin, 3.5 arcmin and 2.1 arcmin respectively and a static crystalline lens position in the three eye models. Different fitting conditions were simulated of the scleral lens 2 (K1 = −0.3 and K2 = −0.4), including central vaults of 50, 100, 150, 200 and 250 µm.

3.3. Simulations of the optical impact of vault changes of vertically decentered SCLs

Fig. 7 shows the results of the MTF in the same way as Fig. 3, but now Lens 1 presenting a vertical decentration of 0.5 mm. In this case, decentration did not cause significant changes of the MTF values for any of the three eye models analyzed, regardless of vergence and vault.

Fig. 8 shows the results of the MTF in the same way as Fig. 7, but the decentered SCL is now Lens 2. As can be seen, Lens 2 decentration of 0.5 mm did not significantly worsen the values of the MTF which presented a behavior as that observed with the same SCL well-centered (Fig. 5). Even for low vergence demands, up to 0.25 D, a slight improvement was seen for the three eye models and all the lens vaults.

4. Discussion

This simulation study shows that the change in the vault of a SCL can induce optical changes that can potentially affect the ocular optical quality. Indeed, vault changes have shown the potential of inducing relevant changes in the optical performance of the combined eye model and contact lens for different vergence demands that ranged from intermediate and to near visual tasks. Therefore, the vault of the SCL over a regular and healthy cornea may have a significant impact on the optical and then potentially on visual performance.

4.1. Simulations of the optical impact of vault changes of centered SCLs

In our simulations, three different eye models with discrepant optical properties within a physiological range were used in order to confirm that the impact of the vault's change could be potentially observed in any type of healthy eye. Vincent et al. [20] evaluated the influence of SCL on both the anterior corneal curvature and the optics, confirming that changes in corneal clearance during an 8-hour period were associated to corneal geometry and high order aberrometry changes. However, the same patient was not evaluated for different scleral lens fittings with different corneal clearances or vaults. Moreover, the impact on intermediate and near visual optics was not analyzed. According to our simulations, the MTF varies for different vergence demands and different spatial frequencies, presenting the best optical performance for the lowest vault and at far distance. However, for vergence demands representing near vision, the optical performance improved with a thicker vault. This may be explained by the changes induced in high order aberrations leading to an increase in the depth of focus, and more specifically by changes in primary spherical aberration. At this point, it should be outlined that controlled changes in primary and secondary spherical aberrations may be beneficial for presbyopes due to the enlargement of the depth of focus that can generate [21,22]. Otchere and colleagues analyzed how the variation of corneal clearance of SCLs can impact far distance visual acuity and comfort in patients with corneal ectasia. They found that a scleral lens fitted considering the

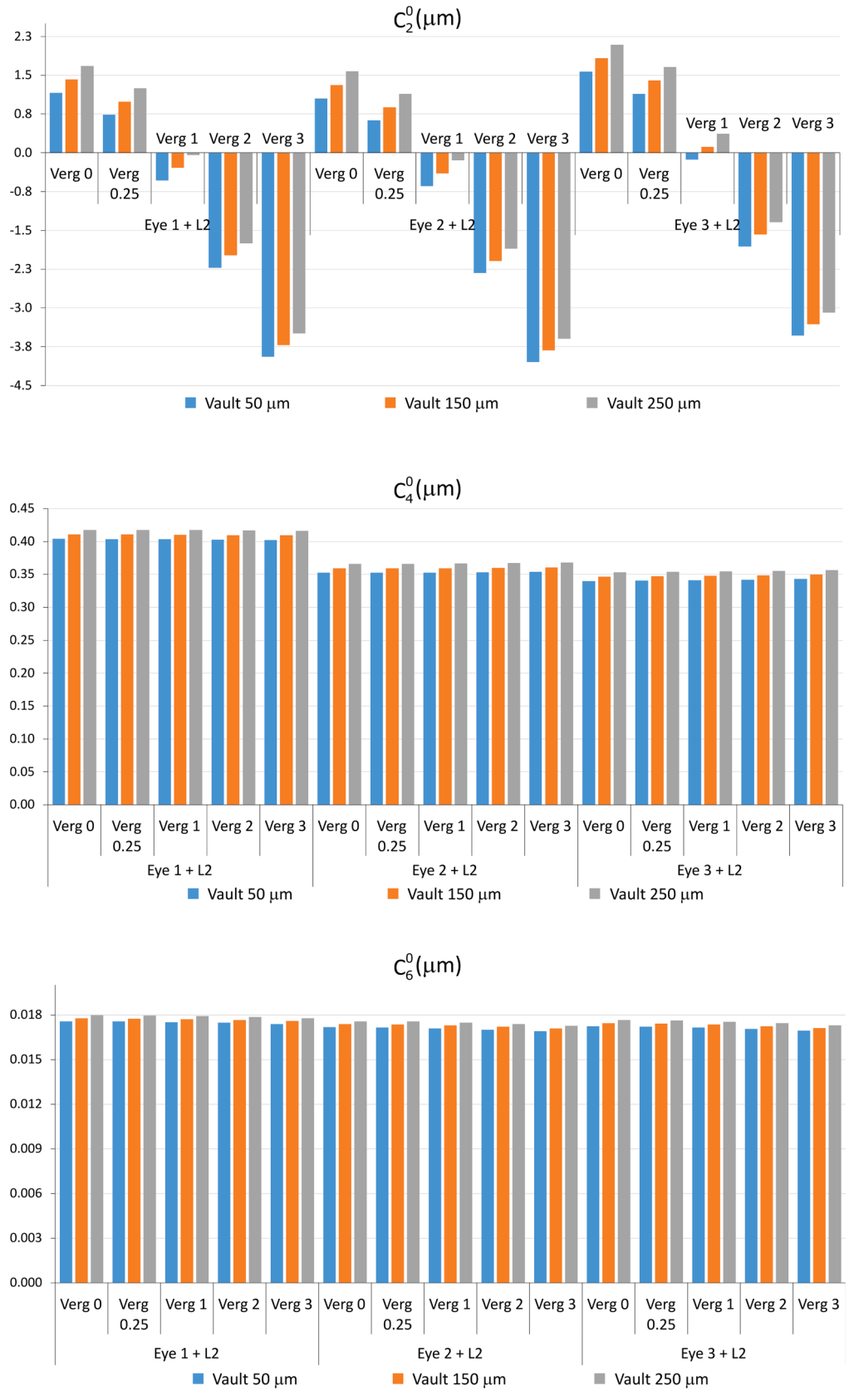

Fig. 6. Zernike coefficients for defocus and primary and secondary spherical aberration of the wavefront error after fitting the scleral contact lens 2 on the three eye models. Different central vaults of the scleral contact lens were used to evaluate the wavefront error at vergence demands ranging from distance to near vision. The crystalline lens remained static in the simulations.

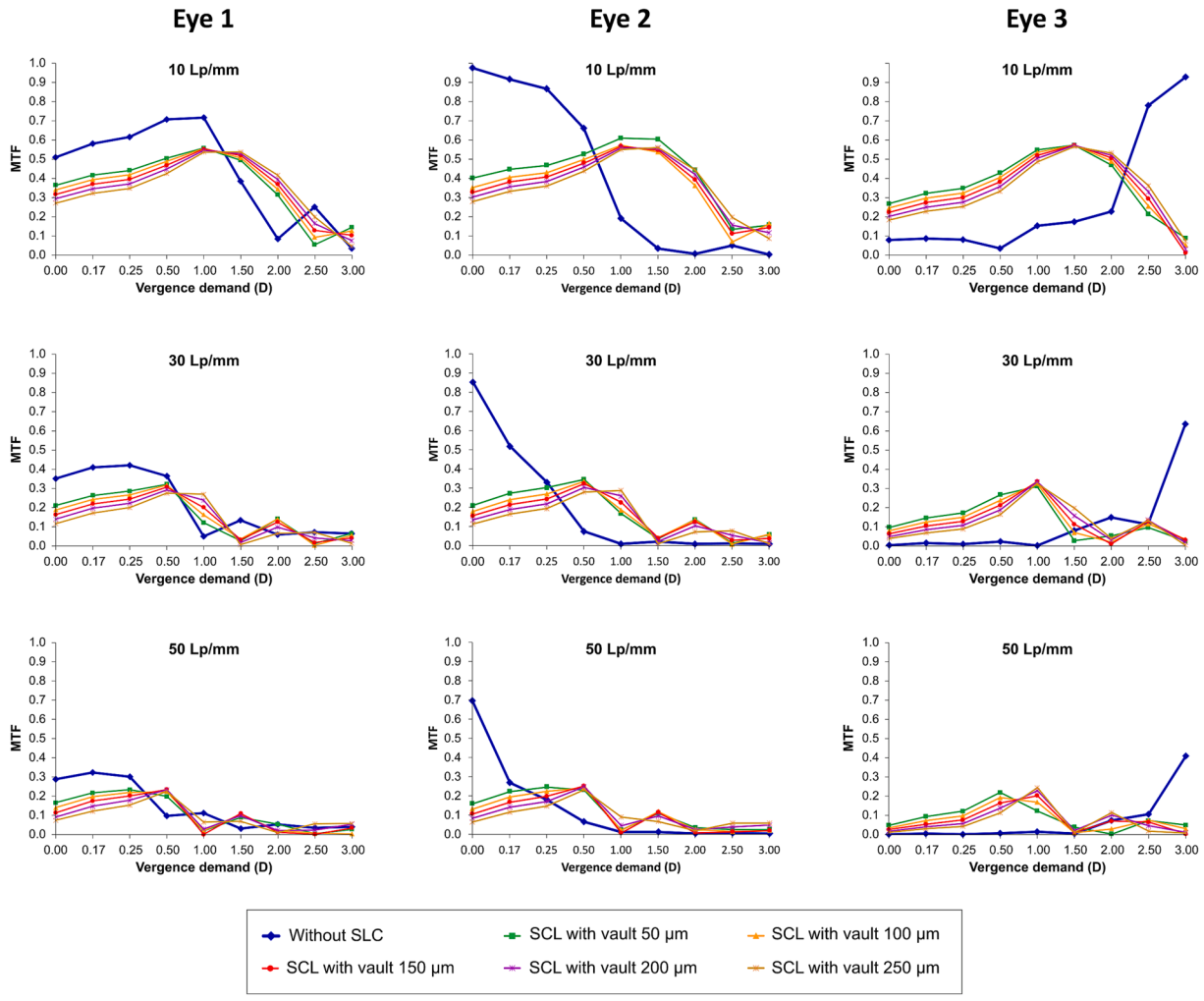

Fig. 7. Modulation transfer function values for different vergence demands after a vertical decentration of 0.5 mm of the scleral contact lens 1. The MTF values were calculated for objects with spatial frequency corresponding to an angular resolution of 10.4 arcmin, 3.5 arcmin and 2.1 arcmin, respectively, and assuming a static crystalline lens position in the three eye models. Different fitting conditions were simulated of the scleral lens 1 (K1 = −0.1 and K2 = −0.4), including central vaults of 50, 100, 150, 200 and 250 µm.

ocular sagittal height, measured with optical coherence tomography at a 15-mm chord on horizontal meridian, and adding 375 µm provided the best combination of acuity and comfort ratings [11].

According to our simulations, there was a trend to increase the level of positive spherical aberration with an increasing vault. Recently, our research group evaluated the aberrometric changes that happened when fitting three models of the same design of SCL but with increasing vault in 15 eyes of 15 patients [12]. Similarly, an increasing positive spherical aberration was found when fitting SCLs with higher vaults, except with the SCL fitted with the highest vault possibly due to the presence of some level of lens flexure as some level of induction of astigmatism was also measured [12]. These clinical results confirm the aberrometric induction and distance visual changes predicted by the simulations. However, the near visual performance was not evaluated in this previous clinical study from our research group and future trials are needed to corroborate the predictions found in this context.

Besides changes in high order aberrations, significant changes in defocus were also observed with increasing vault, as expected. For this reason, an accurate overrefraction is a crucial step in contact lens fitting as the required optical power of the SCL can change significantly depending on the accepted final corneal clearance. In our previous pilot clinical study, an increase in the level of myopia was also observed with an increasing vault. [12] This finding is consistent with the predicted changes in the defocus term obtained in our simulations. [12] Indeed, the largest changes in magnitude in this previous clinical study was found in manifest sphere. In our simulations, the largest change was also observed in the defocus term. This confirms that one of the most probable changes with an increasing vault when fitting SCLs is in the level of spherical correction.

4.2. *Simulations of the optical impact of vault changes of vertically decentered SCLs*

In our previous clinical pilot study, an induction of primary coma was also observed in some cases due to the presence of some level of decentration. For this reason, we have also investigated the impact of a vertical inferior decentration of the SCL, as this type of decentration is the most common when the lens is not well adjusted due to the gravity effect. [18] Nevertheless, the simulations did not reveal relevant changes in the MTF values when a vertical lens decentration of 0.5 mm was induced. It should be considered that the optical power of the lens simulated was zero and therefore the minimal changes obtained were due to the asymmetrical shape of the meniscus. This confirms that the induction of other aberrations such as coma due to SCL decentration are mainly associated to the optical power of the SCL, with minimal contribution of the meniscus shape, considering that the range of potential SCL decentration when performing a good fitting is limited. Vincent et al. [18] found a minimally horizontal and vertical lens

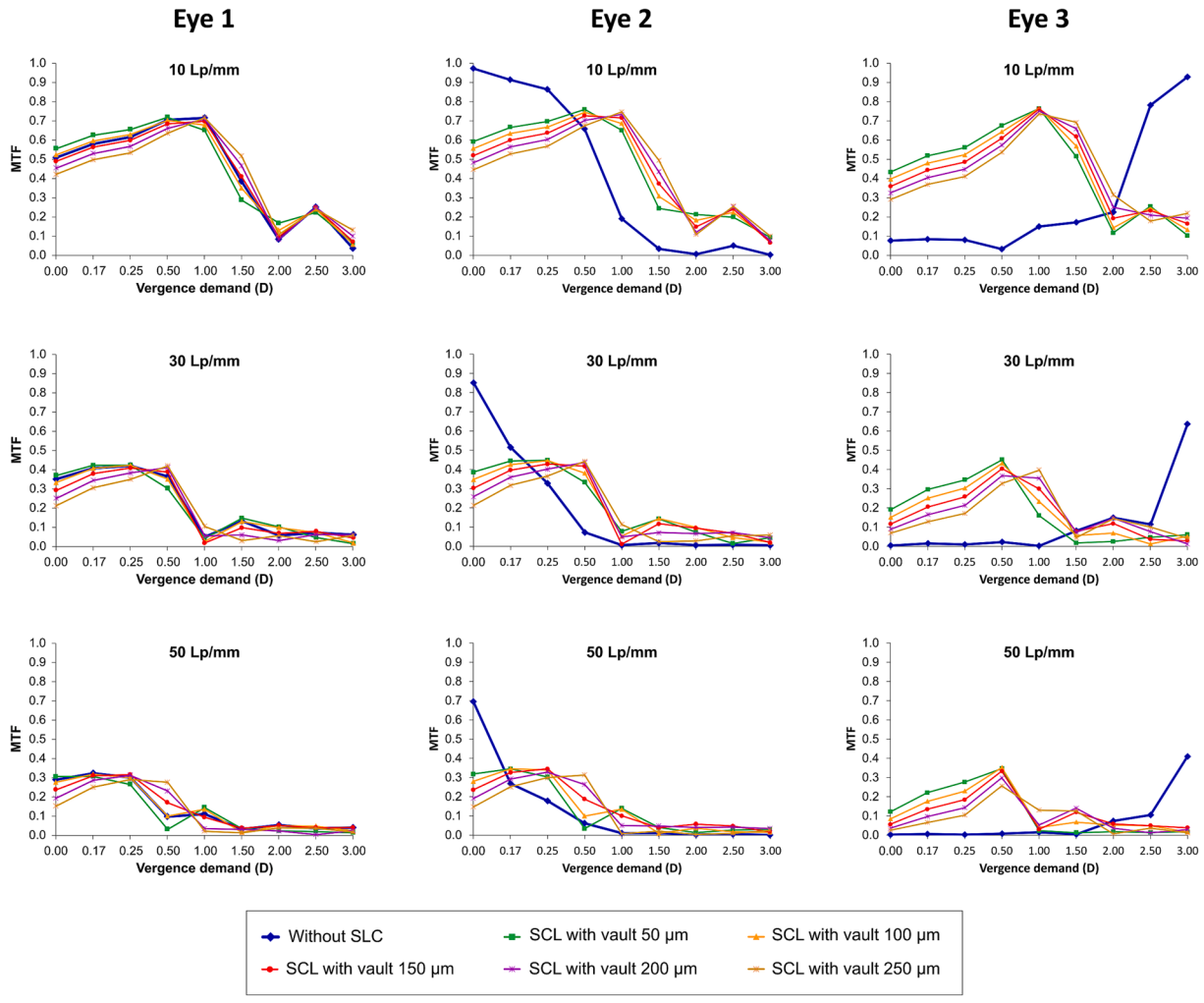

Fig. 8. Modulation transfer function values for different vergence demands after a vertical decentration of 0.5 mm of the scleral contact lens 2. The MTF values were calculated for objects with spatial frequency corresponding to an angular resolution of 10.4 arcmin, 3.5 arcmin and 2.1 arcmin, respectively, and assuming a static crystalline lens position in the three eye models. Different fitting conditions were simulated of the scleral lens 1 (K1 = −0.3 and K2 = −0.4), including central vaults of 50, 100, 150, 200 and 250 µm.

decentration that followed an exponential decay over 8 h that plateaued approximately 2 h after lens insertion and induced a prismatic effect of 0.01 ± 0.16 Δ base out and 0.50 ± 0.19 Δ base down relative to the pupil centre.

4.3. Limitations

This is a simulation study and the results obtained should be considered as potential trends that may be obtained in future clinical studies. Therefore, interpretation of the results must be done with caution. In any case, some of the results obtained in the current simulation study have been recently confirmed in a pilot clinical study conducted by our research group, as previously mentioned. Furthermore, three eye models with different levels of spherical aberration within the physiological range of this parameter in the healthy eye have been used for the simulations in the attempt of covering the potential variations of such optical parameters [23]. More simulation studies should be conducted to investigate the potential trends that can be found in eyes with irregular corneas, such as keratoconus [24], and if an extended depth of focus can be achieved in these eyes when they become presbyopes by the induction of selected levels of high order aberrations. Finally, it should be remarked that accommodation was assumed to be zero in the current simulations, without any change despite modifying the vergence demand. Future simulations should consider the effect of changing accommodation on the optical quality at intermediate and near distances.

5. Conclusions

In conclusion, the simulations performed suggest that the selection of the corneal clearance to be used with a specific model of SCL is crucial not only in terms of oxygen permeability, but also in optical terms as it has the potential of inducing relevant changes in optical quality. According to our simulations, the increase of the vault seems to be associated to a deterioration of the distance visual quality, but an improvement in near visual quality performance. Moreover, the modifications of the vault could be used as a tool to temporarily enlarge the depth of focus in pre-presbyopes or incipient presbyopes, but this should be confirmed in clinical studies.

6. Disclosure

The authors have no proprietary or commercial interest in the medical devices that are involved in this manuscript.

This research was co-funded by Laboratorios Lenticon S.A. and the University of Alicante within the proof-of-concept project PC15-02 “Diseño de lente de contacto escleral multifocal personalizada (Presbycustom).”

The author David P. Piñero has been also supported by the Ministry of Economy, Industry and Competitiveness of Spain within the program Ramón y Cajal, RYC-2016-20471.

Declaration of Competing Interest

The authors declare that they have no known competing financial interests or personal relationships that could have appeared to influence the work reported in this paper.

References

[1] Davies I. Scleral publications & contact lens category growth. Cont Lens Anterior Eye 2019;42:234–5.
[2] Harthan J, Shorter E, Nau C, Nau A, Schornack MM, Zhuang X, et al. Scleral lens fitting and assessment strategies. Cont Lens Anterior Eye 2019;42:9–14.
[3] Harthan J, Nau CB, Barr J, Nau A, Shorter E, Chimato NT, et al. Scleral lens prescription and management practices: the SCOPE study. Eye Contact Lens 2018; 44(Suppl 1):S228–32.
[4] Van der Worp E, Bornman D, Ferreira DL, Faria-Ribeiro M, Garcia-Porta N, González-Meijome JM. Modern scleral contact lenses: a review. Cont Lens Anterior Eye 2014;37:240–50.
[5] Giasson CJ, Morency J, Melillo M, Michaud L. Oxygen tension beneath scleral lenses of different clearances. Optom Vis Sci 2017;94:466–75.
[6] Compañ V, Aguilella-Arzo M, Edrington TB, Weissman BA. Modeling corneal oxygen with scleral gas permeable lens wear. Optom Vis Sci 2016;93:1339–48.
[7] Compañ V, Oliveira C, Aguilella-Arzo M, Mollá S, Peixoto-de-Matos SC, González-Méijome JM. Oxygen diffusion and edema with modern scleral rigid gas permeable contact lenses. Invest Ophthalmol Vis Sci 2014;55:6421–9.
[8] Michaud L, van der Worp E, Brazeau D, Warde R, Giasson CJ. Predicting estimates of oxygen transmissibility for scleral lenses. Cont Lens Anterior Eye 2012;35: 266–71.
[9] Vincent SJ, Alonso-Caneiro D, Collins MJ, Beanland A, Lam L, Lim CC, et al. Hypoxic corneal changes following eight hours of scleral contact lens wear. Optom Vis Sci 2016;93:293–9.
[10] Guillon NC, Godfrey A, Hammond DS. Corneal edema in a unilateral corneal graft patient induced by high Dk mini-scleral contact lens. Cont Lens Anterior Eye 2018; 41:458–62.
[11] Otchere H, Jones L, Sorbara L. The impact of scleral contact lens vault on visual acuity and comfort. Eye Contact Lens 2018;44(Suppl 2):S54–9.
[12] Villa M, Cavas F, Piñero DP. Optical impact of corneal clearance in healthy eyes fitted with scleral contact lenses: a pilot study. J Clin Med 2022;11:3424.
[13] Sonsino J, Mathe DS. Central vault in dry eye patients successfully wearing scleral lens. Optom Vis Sci 2013;90:e248–51.
[14] Vincent SJ, Fadel D. Optical considerations for scleral contact lenses: a review. Cont Lens Anterior Eye 2019;42:598–613.
[15] Woods C, Ruston D, Hough T, Efron N. Clinical performance of an innovative back surface multifocal contact lens in correcting presbyopia. CLAO J 1999;25:176–81.
[16] Thibos LN, Applegate R, Schwiegerling JT, Webb R. Standards for reporting the optical aberrations of eyes. J Refract Surg 2002;18:S652–60.
[17] Escudero-Sanz I, Navarro R. Off-axis aberrations of a wide-angle schematic eye model. J Opt Soc Am A Image Sci Vis 1999;16:1881–91.
[18] Vincent SJ, Alonso-Caneiro D, Collins MJ. The temporal dynamics of miniscleral contact lenses: central corneal clearance and centration. Cont Lens Anterior Eye 2018;41:162–8.
[19] Atchison DA, Scott DH, Charman WN. Hartmann-Shack technique and refraction across the horizontal visual field. J Opt Soc Am A 2003;20:965–73.
[20] Vincent SJ, Alonso-Caneiro D, Collins MJ. Miniscleral lens wear influences corneal curvature and optics. Ophtalmic Physiol Opt 2016;36:100–11.
[21] Benard Y, Lopez-Gil N, Legras R. Optimizing the subjective depth-of-focus with combinations of fourth- and sixth-order spherical aberration. Vision Res 2011;51: 2471–7.
[22] Benard Y, Lopez-Gil N, Legras R. Subjective depth of field in presence of 4th-order and 6th-order Zernike spherical aberration using adaptive optics technology. J Cataract Refract Surg 2010;36:2129–38.
[23] Wang L, Koch DD. Ocular higher-order aberrations in individuals screened for refractive surgery. J Cataract Refract Surg 2003;29:1896–903.
[24] Nilagiri VK, Metlapally S, Schor CM, Bharadwaj SR. A computational analysis of retinal image quality in eyes with keratoconus. Sci Rep 2020;10:1321.